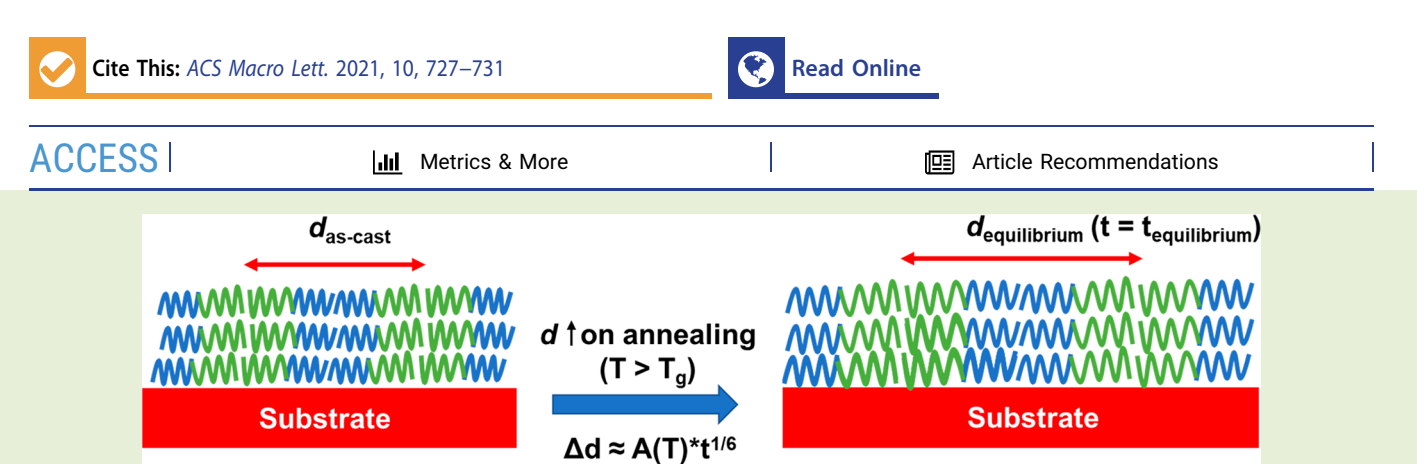


pubs.acs.org/macroletters Letter

# Late Stage Domain Coarsening Dynamics of Lamellar Block Copolymers

Maninderjeet Singh, Wenjie Wu, Vinay Nuka, Joseph Strzalka, Jack F. Douglas,\* and Alamgir Karim\*



**ABSTRACT:** Block copolymer (BCP) phase separation dynamics can be expected to differ significantly from that of the polymer blends due to the constraint of chain connectivity. BCP phase separation dynamics has been studied theoretically, but there has been little experimental evidence to confirm the BCP domain growth scaling laws put forward theoretically. Here, we investigate the dynamics of late-stage lamellar BCP domain coarsening and find that the scaling exponent for lamellar domain growth is  $\approx 1/6$  (0.17), irrespective of the annealing temperature, a value close to the scaling exponent of 0.2 predicted by theoretical studies. Furthermore, we show that the prefactors in the domain coarsening equation show Arrhenius dependence on temperature, indicating that the BCP domain growth dynamics is Arrhenius over the temperature range investigated.

B lock copolymers are a unique class of polymers having two or more chemically distinct polymers joined together by covalent bonds. Due to the difference in the chemical nature of the polymer blocks, block copolymers (BCP) microphase separate into different structures when the enthalpic contribution to the free energy overcomes the entropic contribution in melt state. Diblock copolymers form spherical, cylindrical, gyroid, and lamellar morphologies in the phase-separated state. These morphologies in thin films have found applications in nanolithography, nanoarrays, membranes, and energy storage devices.

The dynamics of microphase separation of block copolymers  $^{12}$  differs significantly as compared to the macrophase separation of polymer blends  $^{13}$  due to the connectivity of polymer chains. The dynamics of macrophase separation of polymer blends has been intensively studied  $^{13,14}$  and involves phase separation by diffusion, followed by a relatively fast phase separation process driven by capillary wave-driven instability. The characteristic length scale follows  $t^{1/3}$  power law in the diffusive regime and a linear growth in time in the hydrodynamic regime at long times.  $^{13,14}$  On the other hand, the picture of microphase separation dynamics of BCPs is far from clear.  $^{15,16}$  A number of theoretical studies have tried to understand the dynamics of the BCP domain structure evolution by microphase separation.  $^{12,17,18}$  On the other hand, there are few experimental studies on validating these predictions. It should be clarified here that there have been

numerous experimental studies on the dynamics of macroscopic BCP grain (comprised of several aligned domains) growth, <sup>19–21</sup> where the kinetics of defect annihilation or reorientation of BCP grains are studied. Our focus in this study is on illustrating the kinetics of microscopic lamellar BCP domain growth, that is, the dynamics of growth of weakly ordered to well-ordered BCP lamellae in their equilibrium state. This is a a process superficially analogous to the polymer blend phase separation, apart from the constraint of chain connectivity that limits the ultimate scale of phase separation. Several theoretical studies have shown the exponents of microscopic domain growth as well, along with the exponents of macroscopic grain growth. <sup>12,17,18</sup>

Shiwa et al. studied the kinetics of phase separation of lamellar BCPs using cell dynamics simulations and observed that the evolution of peak position of the scattering function or domain growth followed a time exponent of 0.2 for weakly segregated BCPs during the late-stage of annealing before reaching its equilibrium value.<sup>12</sup> The authors also observed

Received: February 18, 2021 Accepted: May 21, 2021



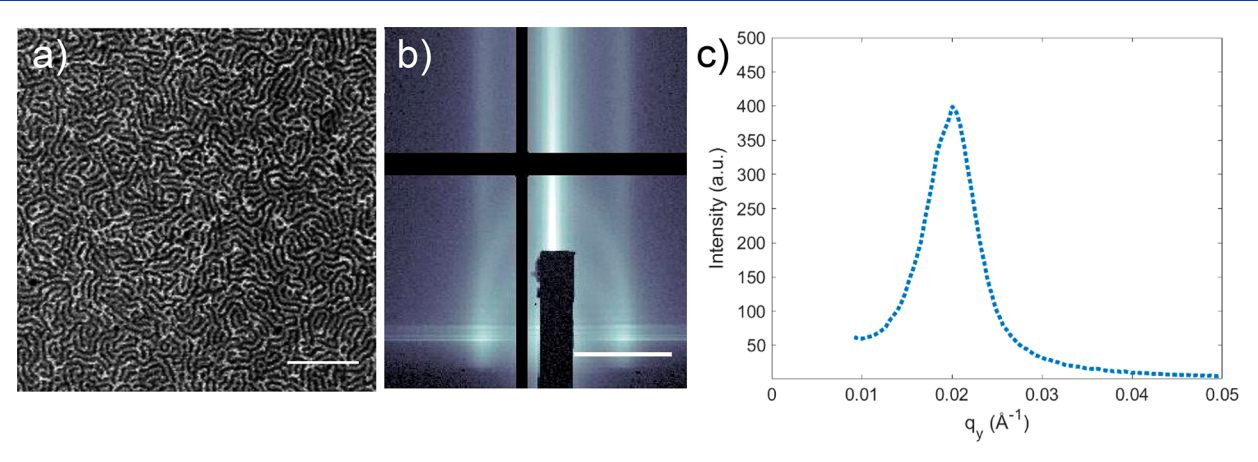


Figure 1. As-cast morphology showing vertical morphology frozen in the nonequilibrium state. (a) AFM image showing as cast morphology. Scale bar corresponds to 400 nm. (b) GISAXS image of the same as-cast morphology showing through thickness morphology. Scale bar corresponds to 0.03 Å<sup>-1</sup>. (c) Line cut along  $q_y$  at Yoneda band showing a peak corresponding to  $d \approx 30.7$  nm.

that the peak width and peak amplitude of the scattering function or the BCP grain size followed exponents of 0.16 and 0.18. These authors furthermore argued that the BCPs and Rayleigh-Bernard convective systems belong to the same "universality class", as they follow the same coarsening exponents. Although the kinetics of grain growth showed a lower coarsening exponent, as compared to the domain growth kinetics, the authors did not delve into the details of the difference between the kinetics of grain growth and lamellar domain growth (termed simply as 'domain growth' below for brevity). The same authors compared the exponents of domain growth in the weakly segregated BCP regime with the strong segregation regime and observed a higher exponent values for strongly segregated BCPs. 18 Other theoretical studies have shown the peak position shift or growth of domains during the early stages of BCP ordering, but the scaling exponents have not been reported for domain growth kinetics. 15,22,23 There has been only one previous experimental study (to the best of our knowledge) to illustrate the domain coarsening kinetics of BCPs. In this study, 16 Russell and Chin followed the evolution of freeze-dried samples of polystyrene-block-poly(methyl methacrylate) (PS-b-PMMA) and observed an exponent of 0.1 for domain coarsening, which is far from the theoretical predictions of the 0.2 exponent. 12 The authors noted that the microvoids in the freeze-dried sample might have influenced their results. Thus, it is a natural question to explore the domain coarsening kinetics of BCPs in solvent cast films that are free of microvoids.

In this study, we have experimentally verified the scaling behavior of domain coarsening kinetics at different temperatures and observe that the as-cast BCP film gets quenched in a nonequilibrium weakly ordered morphology having domain size  $(d \text{ or } L_0)$  smaller than the equilibrium domain size  $(d_{as-cast})$  $< d_{
m equilibrium})$  due to rapid solvent evaporation. The  $d_{
m as-cast}$  BCP domain size grows on annealing the BCP film in the melt state due to the unfavorable interactions between two blocks. We observe that the domain coarsening kinetics follows a transient exponent of 1/6 (that occurs before equilibration at long times), which is rather different from the exponent value 1/3 normally found in polymer blends exhibiting macroscopic phase separation. Furthermore, the prefactors in the domain coarsening power-law follow an Arrhenius temperature dependence, indicating an exponential dependence of the prefactors on temperature.

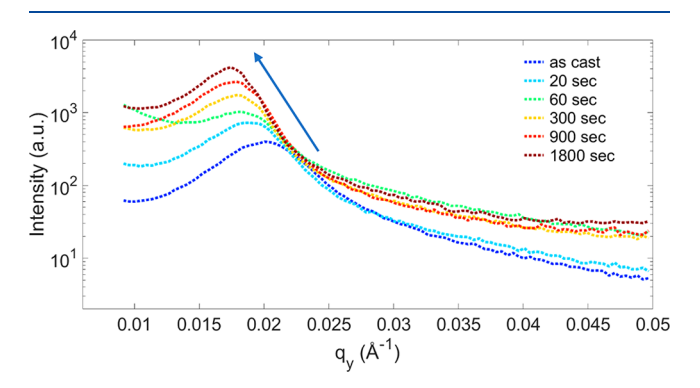
Polystyrene-block-poly(methyl methacrylate) (PS-b-PMMA) BCP used in this study was purchased from Polymer Source and has a molecular mass of 33-b-33 kg/mol. The BCP at this molecular mass has a  $\chi N \approx 23$  and belongs to the weak segregation regime. The BCP films having 100 nm thickness were flow coated on silicon wafers purchased from University Wafers. The Grazing Incidence-small-angle X-ray scattering (GISAXS) studies were conducted at beamline 8-ID-E<sup>25</sup> of the Advanced Photon Source of Argonne National Laboratory and the data were analyzed using GIXSGUI<sup>26</sup> software. The GISAXS measurements were performed on ex-situ annealed samples.

Figure 1 shows the as-cast morphology of PS-b-PMMA films flow coated from tetrahydrofuran (THF) solvent. Due to the rapid evaporation of the casting solvent and a high glass transition temperature ( $T_{\rm e} \approx 105$  °C), the BCP films become vitrified in a non-equilibrium state exhibiting a short-range order with kink-defects. However, the as-cast morphology for these solvent-casting conditions is predominantly vertically oriented, as is evident from the atomic force microscopy (AFM) image in Figure 1a, and the 2D grazing incidence small-angle X-ray scattering (GISAXS) image in Figure 1b. We believe that the evaporation fronts during the film casting are responsible for the as-cast predominantly vertical orientation of the BCP film. The as-cast state of weakly ordered vertical orientation is discussed in more detail in our other work.<sup>31</sup> In the present study, the as-cast well-defined vertical orientation provides a unique opportunity for studying the kinetics of domain coarsening at the early stages of BCP annealing as the focus of our study, wherein the BCPs maintain their vertical morphology over non-treated substrates. The vertical ordering is relatively unconstrained by surface wetting and finite-size effects at the time scales studied here and, hence, provides for a cleaner interpretation of domain growth kinetics as an intrinsic BCP ordering property. However, we note that vertical orientation is not a requirement for validating the power-law exponent of domain growth. Figure 1c shows the GISAXS intensity profile (at a grazing incidence angle of 0.15°, which is above the film critical angle of 0.11°, so the entire depth of the BCP film is measured) along the  $q_v$  direction, showing a welldefined peak indicative of a perpendicular BCP film domain morphology over a large area. The peak position along  $q_{\nu}$ corresponds to 0.0205  $\text{Å}^{-1}$ , which is far from the long-time thermal melt annealed equilibrium peak position of 0.017 Å<sup>-1</sup>.

In real space, the as-cast BCP domain size corresponds to  $\approx 30.7$  nm, while the equilibrium domain size is  $\approx 37$  nm. The lower domain size in the as-cast BCP film is due to the rapid vitrification of the BCP film to its glassy state due to fast solvent evaporation. As noted before, the evaporation front apparently induces vertical orientation and weakly phase-separated BCP morphology, enabling our experimental study of domain coarsening.

When the weakly phase-separated as-cast BCP is annealed above its glass transition temperature, the block copolymers microphase separate further in order to minimize the free energy by minimizing the unfavorable interactions.<sup>27</sup> We studied the evolution of lamellar domain size at different temperatures by analyzing the peak position in GISAXS profiles at different annealing times.

Figure 2 shows the 1D GISAXS line cut along the Yoneda scattering at different annealing times at an annealing



**Figure 2.** Intensity vs q profile showing the effect of annealing on BCP domain size at 180 °C. The peaks shift to lower q (as indicated by the arrow) on annealing, demonstrating an increase of domain size before reaching to equilibrium value ( $d \approx 37$  nm). The peaks are offset to higher intensity arbitrarily with increasing annealing time to show peak shift with q.

temperature of 180 °C, a temperature well above the glass transition temperature of the BCP  $\approx 120$  °C.  $^{28,30}$  The peak position in the  $q_y$  line cuts of the GISAXS images decreases to lower q values with increased annealing times until the peak position reaches the equilibrium peak position of  $\approx 0.017~\text{Å}^{-1}$ . This corresponds to an increase of domain size in real space ( $d=2\pi/q^*$ , where d is the domain size and  $q^*$  is the peak position) with annealing time. This shift of peak position to lower q values is analogous to the observation of lowering of the peak position of the structure factor by Shiwa et al. for weakly segregated BCPs.  $^{12}$  and by Yokojima et al. for weakly, as well as strongly segregated BCPs.  $^{18}$ 

The evolution of domain size in real space as a function of annealing time (t) for three different temperatures is shown in Figure 3. The evolution of domain size is represented as  $\Delta d = A(T)t^n$  in Figure 3, where  $\Delta d$  is the domain size increment/growth, A(T) is a temperature (T)-dependent prefactor, and n is the scaling exponent describing domain coarsening. Interestingly, the time exponent for domain size evolution is independent of annealing temperature and is equal to 0.17  $(\approx 1/6)$ . It should be pointed out here that we have used the domain size growth  $(\Delta d = d_t - d_{t=0})$ , where  $d_t$  is the domain size at time t, making the domain growth equation as  $d_t = d_{t=0} + A(T)t^n$  in calculating the scaling exponents as compared to the other theoretical and experimental studies,  $d_t = d_{t=0} = 0$ . This is because of the finite nonzero domain size of our

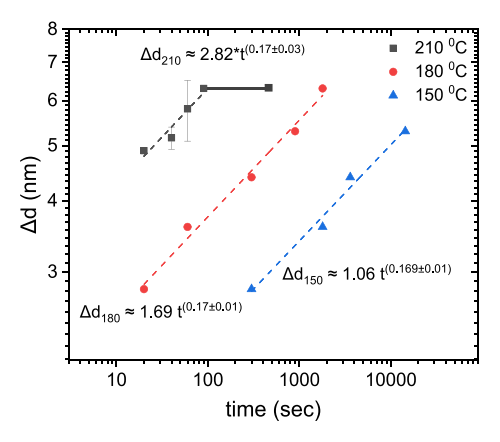


**Figure 3.** Increase of domain size with annealing time at different annealing temperatures. The error bars show the standard deviation. The domain coarsening mechanism follows the same power law coefficient at different temperatures. Dotted lines show best fits to the data points. The solid line shows the saturation of domain size to the equilibrium value. The fitted prefactors of the power-law decrease with temperature.

system at the 'initial' time t = 0, at which we started acquiring data. A slightly higher exponent (n = 0.2) in the growth of latestage block copolymer domain coarsening has been observed in simulation studies of defect-free systems by Shiwa et al. 12 and Yokojima et al. 18 for weakly segregated BCPs, as applicable to our PS-b-PMMA system ( $\chi N \approx 23$ ).<sup>24</sup> Additionally, it has been shown that other systems with reduced degrees of freedom, such as binary mixtures of polymer-tethered nanoparticles, show a scaling exponent of 0.22 for the growth of phase-separated domains, <sup>29</sup> which is close to the observed exponent in our case. The domain size ultimately reaches or approaches the equilibrium value of  $d_{\text{equilibrium}} \approx 37 \text{ nm}$  ( $\Delta d \approx$ 6.3 nm in Figure 3) after different annealing times depending on the temperature, as shown in Figure 3. An abrupt 'pinning' of the domain size at  $\Delta d \approx 6.3$  nm to its long equilibrium value is shown with the horizontal solid line for the highest annealing temperature of 210 °C in Figure 3.

The prefactor A in Figure 3 fitted to the evolution of BCP domains decreases with decreasing temperature as expected. The prefactors (A) for the domain coarsening equation are fitted to an Arrhenius equation  $(A(T) \sim A_0 \exp(-E_a/RT))$  and show a very good fit, as shown in Figure 4, where  $E_a$  is the activation energy and R is the gas constant. The data is plotted as  $\ln(A)$  versus 1/T, with the slope as  $E_a/R$ , with an  $E_a \approx 27.6$ 

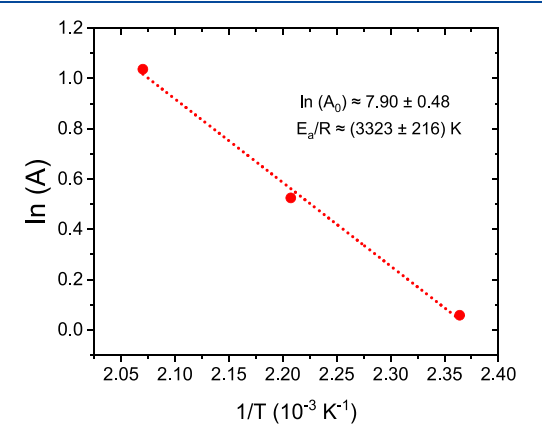


Figure 4. Arrhenius dependence of prefactors on temperature.

kJ/mol and  $A_0 \approx 2690$ . This value of  $E_a$  is much smaller than the  $E_a$  observed in the grain coarsening of BCP during late-stage annealing, which has been shown to be around 8300 kJ/mol for  $\chi N \approx 16.3$  by uniform thermal annealing. The large difference in activation energies reflects the different underlying fundamental mechanisms involved in domain coarsening, a local coarsening process on a scale of order of BCP molecule, versus grain growth, a macroscopic process, often observable with a simple microscope.

To summarize, we have studied the dynamics of (vertically oriented) lamellar BCP domain coarsening by annealing weakly preordered as cast BCP films and observed that the late-stage lamellar BCP domain growth follows a time scaling exponent of  $\approx 1/6$  for a wide range of annealing temperatures. The observed scaling exponent is close to the simulations determined scaling exponent of 0.2 for late-stage domain coarsening. Furthermore, we observe that the prefactor in the domain growth scaling equation follows an Arrhenius temperature dependence. Finally, it would be interesting to compare these scaling exponents for strongly segregated BCPs with  $\chi N > 50$ 

## AUTHOR INFORMATION

# **Corresponding Authors**

Jack F. Douglas — Materials Measurement Laboratory, Material Science and Engineering Division, National Institute of Standards and Technology (NIST), Gaithersburg, Maryland 20899, United States; ⊚ orcid.org/0000-0001-7290-2300; Email: jack.douglas@nist.gov

Alamgir Karim — Department of Chemical and Biomolecular Engineering, University of Houston, Houston, Texas 77204, United States; orcid.org/0000-0003-1302-9374; Email: akarim3@central.uh.edu

# **Authors**

Maninderjeet Singh – Department of Chemical and Biomolecular Engineering, University of Houston, Houston, Texas 77204, United States

Wenjie Wu – Department of Chemical and Biomolecular Engineering, University of Houston, Houston, Texas 77204, United States

Vinay Nuka – Department of Chemical and Biomolecular Engineering, University of Houston, Houston, Texas 77204, United States

Joseph Strzalka — X-ray Science Division, Argonne National Laboratory, Argonne, Illinois 60439, United States;
ocid.org/0000-0003-4619-8932

Complete contact information is available at: https://pubs.acs.org/10.1021/acsmacrolett.1c00105

#### Notes

The authors declare no competing financial interest.

### ACKNOWLEDGMENTS

The work was supported by an award from NSF-DMR 1905996. This research used resources of the Advanced Photon Source, a U.S. Department of Energy (DOE) Office of Science User Facility operated for the DOE Office of Science by Argonne National Laboratory under Contract No. DE-AC02-06CH11357. Certain commercial equipment, instruments, or materials are identified in this paper in order to specify the experimental procedure accurately. Such identification is not intended to imply recommendation or

endorsement by the National Institute of Standards and Technology, nor is it intended to imply that the materials or equipment identified are necessarily the best available for the purpose.

## REFERENCES

- (1) Bates, F.; Fredrickson, G. H. Block Copolymer Thermodynamics: Theory And Experiment. *Annu. Rev. Phys. Chem.* **1990**, *41* (1), 525–557.
- (2) Leibler, L. Theory of Microphase Separation in Block Copolymers. *Macromolecules* **1980**, 13 (6), 1602–1617.
- (3) Bates, F. S.; Fredrickson, G. H. Block Copolymers-Designer Soft Materials. *Phys. Today* **1999**, 52 (2), 32–38.
- (4) Darling, S. B. Directing the Self-Assembly of Block Copolymers. *Prog. Polym. Sci.* **2007**, 32 (10), 1152–1204.
- (5) Ouk Kim, S.; Solak, H. H.; Stoykovich, M. P.; Ferrier, N. J.; de Pablo, J. J.; Nealey, P. F. Epitaxial Self-Assembly of Block Copolymers on Lithographically Defined Nanopatterned Substrates. *Nature* **2003**, 424 (6947), 411–414.
- (6) Doerk, G. S.; Cheng, J. Y.; Singh, G.; Rettner, C. T.; Pitera, J. W.; Balakrishnan, S.; Arellano, N.; Sanders, D. P. Enabling Complex Nanoscale Pattern Customization Using Directed Self-Assembly. *Nat. Commun.* **2014**, *5*, 1–8.
- (7) Luo, Y.; Wang, X.; Zhang, R.; Singh, M.; Ammar, A.; Cousins, D.; Hassan, M. K.; Ponnamma, D.; Adham, S.; Al-Maadeed, M. A. A.; Karim, A. Vertically Oriented Nanoporous Block Copolymer Membranes for Oil/Water Separation and Filtration. *Soft Matter* **2020**, *16*, 9648–9654.
- (8) Liu, T.; Liu, G. Block Copolymers for Supercapacitors, Dielectric Capacitors and Batteries. *J. Phys.: Condens. Matter* **2019**, *31* (23), 233001.
- (9) Singh, M.; Apata, I. E.; Samant, S.; Wu, W.; Tawade, B. V.; Pradhan, N.; Raghavan, D.; Karim, A. Nanoscale Strategies to Enhance the Energy Storage Capacity of Polymeric Dielectric Capacitors: Review of Recent Advances. *Polym. Rev.* **2021**, *0* (0), 1–50.
- (10) Samant, S.; Basutkar, M.; Singh, M.; Masud, A.; Grabowski, C. A.; Kisslinger, K.; Strzalka, J.; Yuan, G.; Satija, S.; Apata, I.; Raghavan, D.; Durstock, M.; Karim, A. Effect of Molecular Weight and Layer Thickness on the Dielectric Breakdown Strength of Neat and Homopolymer Swollen Lamellar Block Copolymer Films. *ACS Appl. Polym. Mater.* **2020**, *2* (8), 3072–3083.
- (11) Masud, A.; Longanecker, M.; Bhadauriya, S.; Singh, M.; Wu, W.; Sharma, K.; Terlier, T.; Al-Enizi, A. M.; Satija, S.; Douglas, J. F.; Karim, A. Ionic Liquid Enhanced Parallel Lamellar Ordering in Block Copolymer Films. *Macromolecules* **2021**, na DOI: 10.1021/acs.macromol.0c02546.
- (12) Shiwa, Y.; Taneike, T.; Yokojima, Y. Scaling Behavior of Block Copolymers in Spontaneous Growth of Lamellar Domains. *Phys. Rev. Lett.* **1996**, *77*, 4378.
- (13) Sung, L.; Karim, A.; Douglas, J. F.; Han, C. C. Dimensional Crossover in the Phase Separation Kinetics of Thin Polymer Blend Films. *Phys. Rev. Lett.* **1996**, *76*, 4368.
- (14) Siggia, E. D. Late Stages of Spinodal Decomposition in Binary Mixtures. *Phys. Rev. A: At., Mol., Opt. Phys.* **1979**, 20 (2), 595–602.
- (15) Song, K. X.; Jia, Y. X.; Sun, Z. Y.; An, L. J. Lattice Boltzmann study of hydrodynamic effects in lamellar ordering process of two-dimensional quenched block copolymers. *J. Chem. Phys.* **2008**, *129*, 144901.
- (16) Russell, T. P.; Chin, I. On the Microphase Separation Kinetics of Symmetric Diblock Copolymers. *Colloid Polym. Sci.* **1994**, 272 (11), 1373–1379.
- (17) Bahiana, M.; Oono, Y. Cell Dynamical System Approach to Block Copolymers. *Phys. Rev. A: At., Mol., Opt. Phys.* **1990**, *41*, 6763.
- (18) Yokojima, Y.; Shiwa, Y. Ordering Process in Quenched Block Copolymers at Low Temperatures. *Phys. Rev. E: Stat. Phys., Plasmas, Fluids, Relat. Interdiscip. Top.* **2000**, *62*, 6838.

- (19) Li, W.; Müller, M. Defects in the Self-Assembly of Block Copolymers and Their Relevance for Directed Self-Assembly. *Annu. Rev. Chem. Biomol. Eng.* **2015**, 6 (1), 187–216.
- (20) Ruiz, R.; Sandstrom, R. L.; Black, C. T. Induced Orientational Order in Symmetric Diblock Copolymer Thin Films. *Adv. Mater.* **2007**, *19* (4), 587–591.
- (21) Harrison, C.; Adamson, D. H.; Cheng, Z.; Sebastian, J. M.; Sethuraman, S.; Huse, D. A.; Register, R. A.; Chaikin, P. M. Mechanisms of Ordering in Striped Patterns. *Science* **2000**, 290 (5496), 1558–1560.
- (22) Maurits, N. M.; Zvelindovsky, A. V.; Sevink, G. J. A.; Van Vlimmeren, B. A. C.; Fraaije, J. G. E. M. Hydrodynamic Effects in Three-Dimensional Microphase Separation of Block Copolymers: Dynamic Mean-Field Density Functional Approach. *J. Chem. Phys.* 1988, 108, 9150.
- (23) Yokojima, Y.; Shiwa, Y. Hydrodynamic Interactions in Ordering Process of Two-Dimensional Quenched Block Copolymers. *Phys. Rev. E: Stat. Phys., Plasmas, Fluids, Relat. Interdiscip. Top.* **2002**, *65*, 056308. (24) Liu, G.; Stoykovich, M. P.; Ji, S.; Stuen, K. O.; Craig, G. S. W.; Nealey, P. F. Phase Behavior and Dimensional Scaling of Symmetric Block Copolymer-Homopolymer Ternary Blends in Thin Films. *Macromolecules* **2009**, *42* (8), 3063–3072.
- (25) Jiang, Z.; Li, X.; Strzalka, J.; Sprung, M.; Sun, T.; Sandy, A. R.; Narayanan, S.; Lee, D. R.; Wang, J. The Dedicated High-Resolution Grazing-Incidence X-Ray Scattering Beamline 8-ID-E at the Advanced Photon Source. *J. Synchrotron Radiat.* **2012**, *19* (4), 627–636.
- (26) Jiang, Z. GIXSGUI: A MATLAB Toolbox for Grazing-Incidence X-Ray Scattering Data Visualization and Reduction, and Indexing of Buried Three-Dimensional Periodic Nanostructured Films. J. Appl. Crystallogr. 2015, 48 (3), 917–926.
- (27) Fredrickson, G. H.; Bates, F. S. Dynamics of Block Copolymers: Theory and Experiment. *Annu. Rev. Mater. Sci.* **1996**, 26 (1), 501–550.
- (28) Basutkar, M. N.; Samant, S.; Strzalka, J.; Yager, K. G.; Singh, G.; Karim, A. Through-Thickness Vertically Ordered Lamellar Block Copolymer Thin Films on Unmodified Quartz with Cold Zone Annealing. *Nano Lett.* **2017**, *17* (12), 7814–7823.
- (29) Schmitt, M.; Zhang, J.; Lee, J.; Lee, B.; Ning, X.; Zhang, R.; Karim, A.; Davis, R. F.; Matyjaszewski, K.; Bockstaller, M. R. Polymer Ligand Induced Autonomous Sorting and Reversible Phase Separation in Binary Particle Blends. Sci. Adv. 2016, 2, No. e1601484. (30) Singh, M.; Basutkar, M.; Samant, S.; Singh, G.; Karim, A. Directed Self-assembly of Block Copolymers with Dynamic Thermal Gradients. Soft Matter and Biomaterials on the Nanoscale; World Scientific, 2020; Chapter 9, pp 373–409, DOI: 10.1142/9789811217982 0009.
- (31) Singh, M.; Wu, W.; Basutkar, M. N.; Strzalka, J.; Al-Enizi, A. M.; Douglas, J. F.; Karim, A. Ultra-Fast Vertical Ordering of Lamellar Block Copolymer Films on Unmodified Substrates. *Macromolecules* **2021**, *54* (3), 1564–1573.